

*This copy is for your personal, non-commercial use only.*

**If you wish to distribute this article to others**, you can order high-quality copies for your colleagues, clients, or customers by [clicking here](#).

**Permission to republish or repurpose articles or portions of articles** can be obtained by following the guidelines [here](#).

**The following resources related to this article are available online at [www.sciencemag.org](http://www.sciencemag.org) (this information is current as of April 30, 2010):**

**Updated information and services**, including high-resolution figures, can be found in the online version of this article at:

<http://www.sciencemag.org/cgi/content/full/327/5969/1132>

**Supporting Online Material** can be found at:

<http://www.sciencemag.org/cgi/content/full/science.1183748/DC1>

A list of selected additional articles on the Science Web sites **related to this article** can be found at:

<http://www.sciencemag.org/cgi/content/full/327/5969/1132#related-content>

This article **cites 25 articles**, 13 of which can be accessed for free:

<http://www.sciencemag.org/cgi/content/full/327/5969/1132#otherarticles>

This article has been **cited by** 3 articles hosted by HighWire Press; see:

<http://www.sciencemag.org/cgi/content/full/327/5969/1132#otherarticles>

This article appears in the following **subject collections**:

Biochemistry

<http://www.sciencemag.org/cgi/collection/biochem>

status. Variation within populations, be it genetic or not, can differ between species in many dimensions that are not documented in species-level data. Species-level analyses fail to capture variation that contributes to diversity if variation among individuals in many dimensions is species-specific. This analysis shows that the massive variation within populations documented in previous studies (4–6) is structured in such a way that it contributes to coexistence.

The explanation that diversity depends on individual variation is consistent with the lack of evidence that individuals recognize the species identities of their competitors. Most competition theory is based on interaction coefficients specific to each species pair, often termed the “community matrix.” This concept has prompted substantial study to quantify interaction strength between species pairs. Neutral theory (22, 23) and the belief that all species are functionally equivalent was partly motivated by the implausibility that plant competition operates differently for each species pair. The individual-level maintenance of biodiversity shown here involves only differences in the ranges of response to the environment and the tendency to respond like conspecifics, and not species-by-species recognition. Those differences translate into differences in individual growth, which determines resource capture, and fecundity, which determines capture of new sites. In contrast to neutral theory, which posits no difference, high diversity is possible because species differ in so many ways. The mechanism demonstrated here is also more general than a rare-species advantage, which invokes host-specific natural enemies (one

to control each species when it becomes abundant) and disappearance of the effect when the host becomes rare (24, 25), or  $N$  natural enemies to explain coexistence of  $N$  hosts. The tendency to respond like other individuals of the same species can promote coexistence independent of local frequency or density and does not require a large number of host-specific enemies.

The biodiversity paradox of many coexisting competitors in which the number of limiting resources seems low can be resolved at the individual level. Just as variation among individuals is required to maintain species by natural selection, providing a means for adaptive evolution in response to many factors in many dimensions, variation at the individual scale is also needed to explain why large numbers of intensely competing species coexist. Individual-level variation need not be genetic (although genotypic variation can be large), but species do need to differ in how individuals respond in many dimensions. In the absence of precise information on the many dimensions in which species differ, individual-level data provide evidence for species differences.

#### References and Notes

1. G. E. Hutchinson, *Am. Nat.* **95**, 137 (1961).
2. M. Rees, R. Condit, M. Crawley, S. Pacala, D. Tilman, *Science* **293**, 650 (2001).
3. J. Silvertown, *Trends Ecol. Evol.* **19**, 605 (2004).
4. J. S. Clark, S. LaDeau, I. Ibanez, *Ecol. Monogr.* **74**, 415 (2004).
5. J. S. Clark *et al.*, *Ecol. Lett.* **10**, 647 (2007).
6. J. E. Mohan, J. S. Clark, W. H. Schlesinger, *Ecol. Appl.* **17**, 1198 (2007).
7. R. Condit *et al.*, *Science* **313**, 98 (2006); published online 8 June 2006 (10.1126/science.1124712).

8. J. S. Clark, J. S. McLachlan, *Nature* **423**, 635 (2003).
9. J. S. Clark *et al.*, in *Handbook of Bayesian Analysis*, T. O'Hagan, M. West, Eds. (Oxford Univ. Press, New York, 2010), pp. 431–481.
10. Materials and methods are available as supporting material on *Science* Online.
11. R. H. MacArthur, R. Levins, *Proc. Natl. Acad. Sci. U.S.A.* **51**, 1207 (1964).
12. S. A. Levin, *Am. Nat.* **104**, 413 (1970).
13. D. Tilman, *Plant Strategies and the Dynamics and Structure of Plant Communities* (Princeton Univ. Press, Princeton, NJ, 1988).
14. D. Tilman, *Proc. Natl. Acad. Sci. U.S.A.* **101**, 10854 (2004).
15. D. Gravel, C. D. Canham, M. Beaudet, C. Messier, *Ecol. Lett.* **9**, 399 (2006).
16. T. Zillio, R. Condit, *Oikos* **116**, 931 (2007).
17. R. Levins, *Am. Nat.* **114**, 765 (1979).
18. P. Chesson, *Annu. Rev. Ecol. Syst.* **31**, 343 (2000).
19. P. B. Adler, J. HilleRisLambers, P. C. Kyriakidis, Q. Guan, J. M. Levine, *Proc. Natl. Acad. Sci. U.S.A.* **103**, 12793 (2006).
20. A. L. Angert, T. E. Huxman, P. Chesson, D. L. Venable, *Proc. Natl. Acad. Sci. U.S.A.* **106**, 11641 (2009).
21. N. McDowell *et al.*, *New Phytol.* **178**, 719 (2008).
22. S. P. Hubbell, *The Unified Neutral Theory of Biodiversity and Biogeography* (Princeton Univ. Press, Princeton, NJ, 2001).
23. S. P. Hubbell, *Ecology* **87**, 1387 (2006).
24. D. H. Janzen, *Am. Nat.* **104**, 501 (1970).
25. J. H. Connell, in *Dynamics of Numbers in Populations*, P. J. Boer, G. R. Graadwell, Eds. (Centre for Agricultural Publishing and Documentation, Wageningen, Netherlands, 1971), pp. 298–312.

#### Supporting Online Material

www.sciencemag.org/cgi/content/full/327/5969/1129/DC1  
Materials and Methods

Figs. S1 to S3

Tables S1 to S3

References

19 October 2009; accepted 18 January 2010

10.1126/science.1183506

## Generating a Prion with Bacterially Expressed Recombinant Prion Protein

Fei Wang,<sup>1\*</sup> Xinhe Wang,<sup>1\*</sup> Chong-Gang Yuan,<sup>2</sup> Jiyan Ma<sup>1,2,†</sup>

The prion hypothesis posits that a misfolded form of prion protein (PrP) is responsible for the infectivity of prion disease. Using recombinant murine PrP purified from *Escherichia coli*, we created a recombinant prion with the attributes of the pathogenic PrP isoform: aggregated, protease-resistant, and self-perpetuating. After intracerebral injection of the recombinant prion, wild-type mice developed neurological signs in ~130 days and reached the terminal stage of disease in ~150 days. Characterization of diseased mice revealed classic neuropathology of prion disease, the presence of protease-resistant PrP, and the capability of serially transmitting the disease; these findings confirmed that the mice succumbed to prion disease. Thus, as postulated by the prion hypothesis, the infectivity in mammalian prion disease results from an altered conformation of PrP.

**T**ransmissible spongiform encephalopathies (TSEs or prion disease) are infectious neurodegenerative disorders. The prion hypothesis (1) proposes that the infectious agent is an aberrant conformational isoform of the normal PrP (PrP<sup>C</sup>), a glycosylphosphatidylinositol (GPI)-anchored glycoprotein. By virtue of its self-perpetuating characteristic, the aberrant isoform (PrP<sup>Sc</sup>) converts host PrP<sup>C</sup> into the PrP<sup>Sc</sup> con-

formation and leads to neurodegeneration (2–4). Despite strong supporting evidence (5–11), a crucial prediction derived from the prion hypothesis—that an infectious prion can be generated with bacterially expressed recombinant PrP (recPrP)—remains unfulfilled (2, 12), leaving lingering doubts about the prion hypothesis (13).

Recombinant PrP has been folded into various forms similar to PrP<sup>Sc</sup>, but none of them fully

recapitulates the characteristics of the infectious agent (2, 12). The amyloid fiber of a recPrP fragment (recPrP89-230) causes prion disease in transgenic mice overexpressing PrP89-231 (10), but a prolonged incubation time in mice overexpressing PrP has led to uncertainty about whether the infectivity is indeed derived from recPrP89-230 amyloid fibers (2, 12). The difficulty in creating a recombinant prion is likely due to the lack of proper facilitating factors (14). Polyanions, particularly RNA, have been found to facilitate PrP conversion and promote de novo prion formation (9, 15–17). We investigated lipid as a potential facilitating factor because GPI-anchored PrP<sup>C</sup> is in the vicinity of lipid membranes and the interfacial lipid bilayer region strongly influences protein structure (18). Encouraged by the findings that lipid interaction converts recPrP to a PrP<sup>Sc</sup>-like form (19), we applied protein misfolding cyclic amplification (PMCA) (8) to study recPrP

<sup>1</sup>Department of Molecular and Cellular Biochemistry, Ohio State University, Columbus, OH 43210, USA. <sup>2</sup>School of Life Science, East China Normal University, Shanghai 200062, China.

\*These authors contributed equally to this work.

†To whom correspondence should be addressed. E-mail: ma.131@osu.edu

conversion in the presence of both lipid and RNA.

Using a serial PMCA protocol (20), we tested 16 different conditions in which recPrP was mixed with various combinations of lipids and/or total RNA isolated from normal mouse liver. In the presence of the synthetic anionic phospholipid POPG (1-palmitoyl-2-oleoylphosphatidylglycerol) and RNA, a 15-kD proteinase K (PK)-resistant band was detected after 17 rounds of PMCA (Fig. 1A). Once formed, the PK-resistant recPrP (rPrP-res) was able to serially propagate (Fig. 1A and fig. S1). The same procedure was repeated several times, and the overall efficiency of de novo rPrP-res formation was found to be ~20% (fig. S2).

Serial PK-digestion of rPrP-res revealed that the PK-resistant band was detectable after digestion with high concentrations of PK (200 µg/ml; PK:recPrP molar ratio > 50:1) (Fig. 1B). After centrifugation, the rPrP-res was detected only in the pellet fraction (Fig. 1C); moreover, the 15-kD PK-resistant band was not recognized by the 8B4 antibody, which detects an N-terminal epitope of PrP (21) (Fig. 1C). These findings show that, similar to PrP<sup>Sc</sup>, rPrP-res is aggregated, is PK-resistant, and contains a C-terminal PK-resistant core.

Next, we performed PMCA and cell culture analyses to determine whether rPrP-res could seed glycosylated and GPI-anchored endogenous PrP<sup>C</sup>. With normal mouse brain homogenate as substrate, PMCA was carried out with or without

rPrP-res seed. The PK-resistant endogenous PrP, as demonstrated by higher molecular weights of glycosylated PrP, was detected in samples seeded with rPrP-res (Fig. 1D). In reactions without rPrP-res seed, no PK-resistant PrP was detected, allowing us to rule out de novo PrP-res formation or insufficient PK digestion. The cell infection assay was performed on SN56 cells, a murine neuronal cell line susceptible to prion infection (22). Endogenous PrP<sup>C</sup> in SN56 cells was glycosylated and sensitive to PK digestion (Fig. 1E). After rPrP-res infection, the PK-resistant endogenous PrP was detected in cells after 2 passages and remained detectable after 17 passages (Fig. 1E). A similar experiment revealed that the rPrP-res-converted normal mouse brain homogenate (Fig. 1D) could infect SN56 cells as well (fig. S3). Thus, rPrP-res is able to propagate its PK-resistant conformation to endogenous PrP<sup>C</sup>.

To determine whether rPrP-res was capable of causing bona fide prion disease, we infected 8-week-old female CD-1 mice by intracerebral injection. The rPrP-res (inoculum 4) was prepared by propagating rPrP-res through 24 rounds of PMCA. All PMCA products were pooled together and centrifuged through a sucrose cushion. The pellet was washed, resuspended, and used for inoculation. Three control inocula were used for animal study (Table 1). Inoculum 1, consisting of all the components used for rPrP-res propagation except for recPrP and rPrP-res seed, was subjected to the same treatments as inoculum 4. Inoculum 2, consisting of all the components of rPrP-res propagation except for rPrP-res seed, was incubated at 37°C for 24 days without sonication and subjected to the same pelleting and washing treatments. Omitting the sonication step prevented the de novo rPrP-res formation in this control sample, as confirmed by the PK digestion analysis described below (Fig. 2A). Inoculum 3 was prepared by directly mixing recPrP, POPG, and RNA in the inocu-

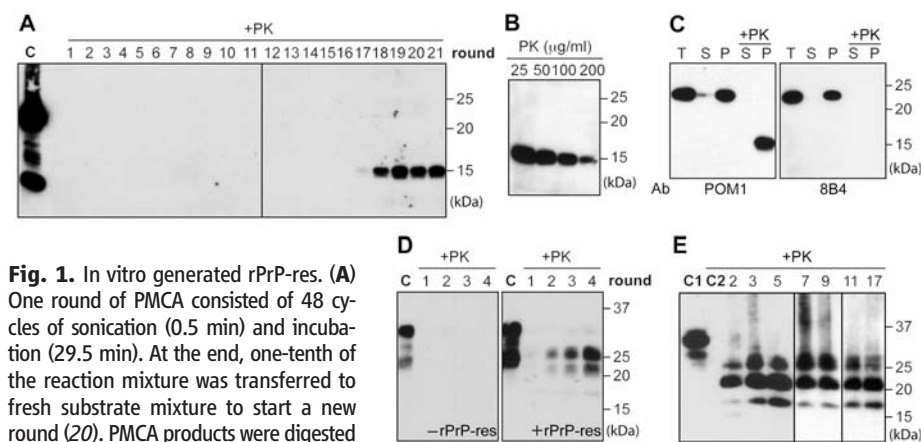


**Fig. 1.** In vitro generated rPrP-res. **(A)** One round of PMCA consisted of 48 cycles of sonication (0.5 min) and incubation (29.5 min). At the end, one-tenth of the reaction mixture was transferred to fresh substrate mixture to start a new round (20). PMCA products were digested with PK (25 µg/ml); C, undigested recPrP. **(B)** Serial PK digestion of PMCA products. **(C)** PMCA product was separated into supernatant (S) and pellet (P) by a 1-hour 100,000g centrifugation at 4°C. T, total input; +PK, digested with PK (25 µg/ml). **(D)** With normal mouse brain homogenate (NMBH) as substrate, PMCA was performed with or without rPrP-res seed. Product was digested with PK (100 µg/ml); C, undigested NMBH. **(E)** After rPrP-res infection, SN56 cells were lysed, digested with PK (25 µg/ml), and centrifuged. The PK-resistant PrP in the pellet was detected by immunoblot analysis. Numbers indicate cell passages. C1, undigested SN56 cell lysate; C2, pellet of PK-digested, uninfected SN56 cell lysates. In all panels, PrP was detected by immunoblot analysis with POM1 antibody to PrP except for the right panel of (C), where 8B4 antibody was used. PK digestion was carried out at 37°C for 30 min [(A), (B), and (C)] or 1 hour [(D) and (E)].

**Table 1.** Intracerebral inoculation of rPrP-res.

Inoculum	Component	Processing	Preparation for injection	Diseased/inoculated	Survival time (dpi)*
1	Buffer + POPG + RNA (the amount of each component equaled that in the rPrP-res propagation reaction)	Serial PMCA	Pelleting through a sucrose cushion and washing twice with PBS	0/15	>360
2	Buffer + POPG + RNA + recPrP (the amount of each component equaled that in the rPrP-res propagation reaction)	Incubated at 37°C without sonication	Pelleting through a sucrose cushion and washing twice with PBS	1†/14	>360 (286†)
3	POPG + RNA + recPrP (the amount of each component equaled that in the final pool of inoculum 4)	No processing	No preparation	0/5	>360
4 (rPrP-res)	Buffer + POPG + RNA + recPrP + rPrP-res seed	Serial PMCA	Pelleting through a sucrose cushion and washing twice with PBS	15/15	150 ± 2.2 (mean ± SEM)

\*One mouse from each group was euthanized at 275 dpi to serve as controls.

†One mouse died from an unrelated disease at 286 dpi. It had no neurological signs or weight loss.

lum diluent. The amount of each component was equal to the total amount in the final pool of inoculum 4, ensuring that the result was not influenced by insufficient dosage of recPrP or any other component. The inoculation and animal care were carried out in an animal vivarium that had never been exposed to animals with prion disease.

After the injection, the remaining inocula were analyzed (Fig. 2A). Inoculum 1 did not contain PrP, and, accordingly, no PrP was detected. Of three inocula that contained recPrP, inoculum 4 had the lowest amount of recPrP (Fig. 2A). However, the 15-kD PK-resistant band was detected only in inoculum 4; hence, it was the only inoculum containing rPrP-res.

Around 130 days post-inoculation (dpi), all 15 rPrP-res-inoculated mice developed clinical signs of prion disease. The earliest sign was clamping, an indication of neurological dysfunction (Fig. 2B). Soon after that, mice developed tail plasticity and akinesia—that is, they remained stationary in response to external stimuli (Fig. 2B and movie S1). The disease progressed rapidly; mice developed kyphosis, head twitching, and mild ataxia, and eventually they became cachexic and lethargic (Fig. 2B and movie S2). The rPrP-res-inoculated mice reached the terminal stage at 136 to 161 dpi, with an average survival time of  $150 \pm 2.2$  days (mean  $\pm$  SEM) (Table 1 and fig. S4). None of the mice injected with control inocula developed prion disease after more than 360 days. Thus, intracerebral rPrP-res injection caused neurodegenerative disorders in wild-type mice, and infectivity was specifically associated with the rPrP-res conformation.

To ensure that every rPrP-res-inoculated mouse received both pathological and biochemical analyses, we bisected each mouse brain sagittally and subjected brain halves to histological or biochemical analysis. Severe spongiosis was detected in multiple brain regions (figs. S5 and S6). Dense small vacuoles were observed in the frontal cortex and caudate nucleus (Fig. 3B and fig. S6), whereas larger vacuoles were detected in the pons, midbrain (areas around raphe nuclei and periaqueductal gray), and cerebellar white matter (areas around cerebellar dentate and fastigial nuclei). Moderate spongiosis was present in the occipital cortex, thalamus, medulla, and hippocampus, whereas little spongiosis was detected in the superior or inferior colliculus, hypothalamus, or olfactory bulb (figs. S6 and S7). Prominent astrogliosis and microgliosis were detected in rPrP-res-inoculated mouse brains (Fig. 3D and fig. S8). PrP immunohistochemistry revealed abnormal PrP deposition in a pattern similar to the diffuse synaptic accumulation (Fig. 3F). The densest PrP deposition was in the thalamus (fig. S8), a finding supported by paraffin-embedded tissue blot (PET blot) analysis (fig. S9). Collectively, rPrP-res-inoculated mouse brains exhibited the classic neuropathological features of prion dis-

ease: spongiosis, astrogliosis, microgliosis, and abnormal PrP deposition.

To determine whether PrP<sup>Sc</sup> was specifically present in rPrP-res-inoculated mice, we euthanized one mouse from each control group at 275 dpi. PrP<sup>Sc</sup> was detected in the rPrP-res-inoculated mouse brain but not in any other control brains (Fig. 3G). Histological analysis confirmed that there was no spongiosis in the control mice. The glycosylation and the electrophoretic pattern of PrP<sup>Sc</sup> were similar among all 15 mice (fig. S10), in agreement with the similar neuropathology

and relatively synchronized disease onset observed among these mice.

To determine whether the rPrP-res-induced disease could be serially transmitted, we prepared 1% brain homogenates from six diseased mice and inoculated each sample intracerebrally into four or five wild-type CD-1 mice. Around 130 dpi, all mice ( $n = 29$ ) developed disease, and the behavior phenotypes were essentially the same as those of the rPrP-res-inoculated mice (movie S3). These mice reached the terminal stage of disease at 151 to 180 dpi; the average survival

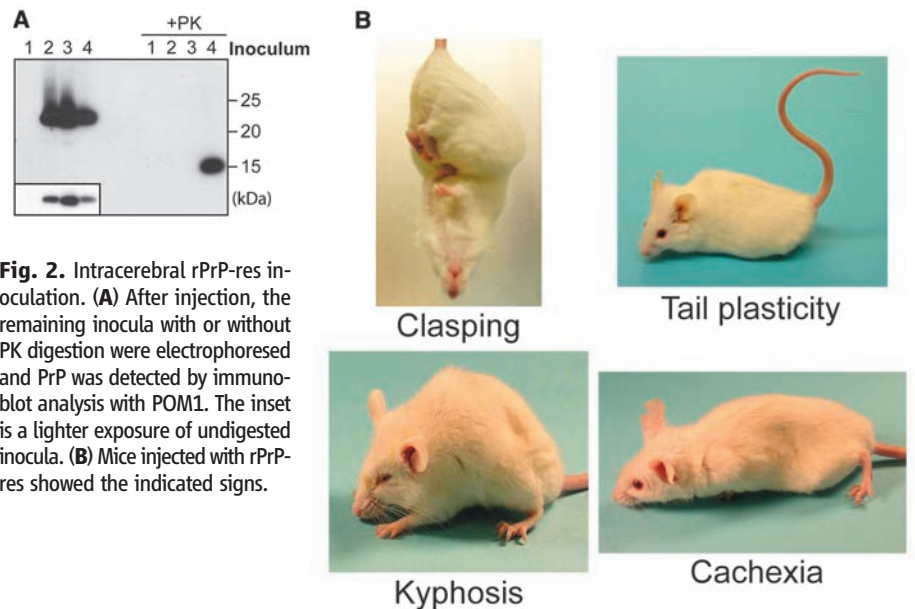


**Fig. 2.** Intracerebral rPrP-res inoculation. (A) After injection, the remaining inocula with or without PK digestion were electrophoresed and PrP was detected by immunoblot analysis with POM1. The inset is a lighter exposure of undigested inocula. (B) Mice injected with rPrP-res showed the indicated signs.

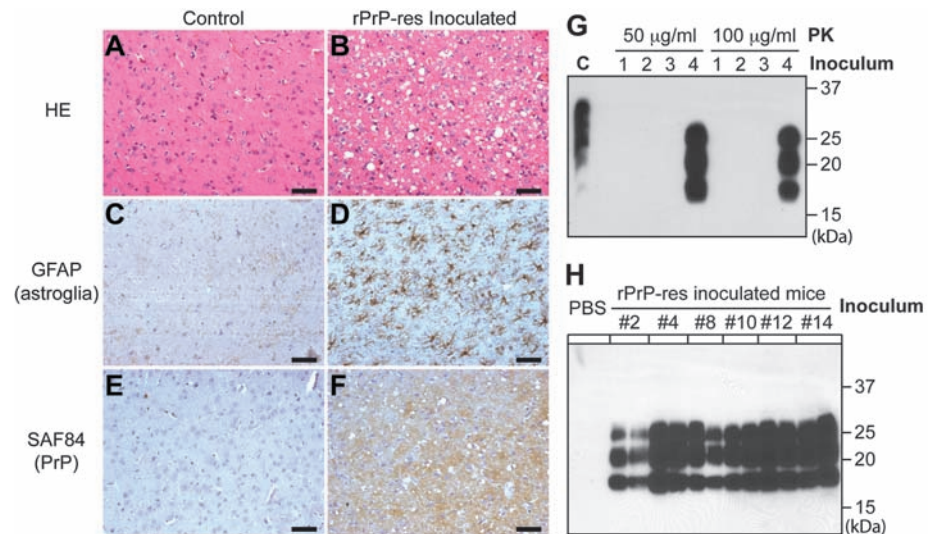


**Fig. 3.** Characterization of rPrP-res-caused prion disease. (A to F) Histological analyses of age- and sex-matched control mice [(A), (C), and (E)] and rPrP-res injected mice [(B), (D), and (F)]. Brain sections were stained by hematoxylin and eosin [(A) and (B)], an antibody to GFAP [glial fibrillary acidic protein] [(C) and (D)], and SAF84 antibody to PrP [(E) and (F)]. Immunohistochemical stains were counterstained with hematoxylin. Scale bars, 50  $\mu$ m. (G) Brain homogenates of an rPrP-res-inoculated mouse or mice inoculated with control inocula 1 to 3 were digested at 37°C for 1 hour with the indicated concentrations of PK. PrP was detected by immunoblot analysis with M20 antibody to PrP. (H) Brain homogenates of mice that received second-round transmission or control mice inoculated with inoculum diluent [phosphate-buffered saline (PBS)] were digested by PK (50  $\mu$ g/ml) at 37°C for 1 hour. PrP was detected by immunoblot analysis with POM1 antibody to PrP. Number indicates the mouse from which the inocula were prepared.

time was  $166 \pm 1.5$  days (fig. S11). The marginal increase in the survival time of second-round transmission could be due to the reported variation among inoculation experiments (23) or to the influence of other components in the brain homogenate used in second-round transmission. Nonetheless, PrP<sup>Sc</sup> was detected in all groups of mice inoculated with diseased mouse brain homogenates, but not in control mice (Fig. 3H). The spongiosis pattern remained similar to that of rPrP-res-inoculated mice (fig. S12). Thus, similar to natural prion disease, the rPrP-res-caused disease can be serially transmitted.

Inadvertent contamination is always a concern for PMCA. The only naturally occurring prion used in our lab was the RML strain, which was used only three times in our failed attempts to convert recPrP. During the past 2 years while we were working with rPrP-res, absolutely no naturally occurring prion was used. Our latest de novo rPrP-res formation (fig. S2) was achieved in a new sonicator, and the substrate was prepared in a lab that has never been exposed to prion. Furthermore, both the behavioral and pathological phenotypes of rPrP-res-inoculated mice were clearly different from those reported for RML-infected mice (24). Thus, it is highly unlikely that rPrP-res formation was due to an inadvertent contamination. Note also that before the inoculum was prepared, the rPrP-res had been propagated for more than 35 rounds of PMCA. Thus, even if the initial rPrP-res formation were due to contamination, the  $>10^{35}$  dilution had ensured that recPrP was the only PrP in the inoculum (Fig. 2A). We therefore conclude that the disease-causing agent was rPrP-res.

The three main components in our system were recPrP, POPG, and RNA. The purity of recPrP was verified by silver staining, and recPrP

was the only protein detected (fig. S13). The mouse liver RNA was chosen because PrP is not normally expressed in liver and because ectopic PrP expression in the liver of PrP-null mice does not support prion propagation (25). Because synthetic polyanions that do not encode protein can replace RNA in cell-free prion formation and propagation (9, 16, 17), the likely role of RNA in generating infectious prions is to facilitate PrP conversion rather than to encode an infectious protein. Indeed, we were able to propagate rPrP-res with the use of synthetic polyadenylated RNA (fig. S14), which shows that rPrP-res can be generated with virtually completely defined components. The requirement of lipid is in accordance with previous reports of higher prion infectivity in lipid membrane-associated PrP<sup>Sc</sup> (22, 26). Notably, the purified GPI-anchored PrP<sup>C</sup>, which was used to produce infectious prion de novo (9), contained stoichiometric amounts of copurified lipids, supporting a general role of lipid in PrP conversion. Of note, the POPG and RNA used here may simply mimic one or more unknown in vivo facilitating factors. Further studies are required to identify these factors.

Our results provide direct evidence in support of the prion hypothesis. We found that rPrP-res is in a conformational state similar to the pathogenic PrP<sup>Sc</sup> isoform, that rPrP-res possesses the self-perpetuating characteristic of a prion, and that rPrP-res causes bona fide prion disease in wild-type mice. The fact that only rPrP-res-inoculated mice developed prion disease establishes that prion disease is caused by the altered conformational form of PrP.

#### References and Notes

1. S. B. Prusiner, *Science* **216**, 136 (1982).
2. B. Caughey, G. S. Baron, B. Chesebro, M. Jeffrey, *Annu. Rev. Biochem.* **78**, 177 (2009).

3. A. Aguzzi, F. Baumann, J. Bremer, *Annu. Rev. Neurosci.* **31**, 439 (2008).
4. J. Collinge, A. R. Clarke, *Science* **318**, 930 (2007).
5. H. Büeler, *Cell* **73**, 1339 (1993).
6. D. A. Kocisko et al., *Nature* **370**, 471 (1994).
7. R. A. Bessen et al., *Nature* **375**, 698 (1995).
8. J. Castilla, P. Saá, C. Hetz, C. Soto, *Cell* **121**, 195 (2005).
9. N. R. Deleault, B. T. Harris, J. R. Rees, S. Supattapone, *Proc. Natl. Acad. Sci. U.S.A.* **104**, 9741 (2007).
10. G. Legname et al., *Science* **305**, 673 (2004).
11. G. C. Telling et al., *Science* **274**, 2079 (1996).
12. C. Weissmann, *Cell* **122**, 165 (2005).
13. L. Manuelidis, *J. Cell. Biochem.* **100**, 897 (2007).
14. B. Caughey, G. S. Baron, *Nature* **443**, 803 (2006).
15. N. R. Deleault, R. W. Lucassen, S. Supattapone, *Nature* **425**, 717 (2003).
16. N. R. Deleault et al., *J. Biol. Chem.* **280**, 26873 (2005).
17. J. C. Geoghegan et al., *J. Biol. Chem.* **282**, 36341 (2007).
18. S. H. White, A. S. Ladokhin, S. Jayasinghe, K. Hristova, *J. Biol. Chem.* **276**, 32395 (2001).
19. F. Wang et al., *Biochemistry* **46**, 7045 (2007).
20. See supporting material on Science Online.
21. T. Pan et al., *J. Virol.* **79**, 12355 (2005).
22. G. S. Baron, A. C. Magalhães, M. A. Prado, B. Caughey, *J. Virol.* **80**, 2106 (2006).
23. G. Tamgüney et al., *J. Gen. Virol.* **89**, 1777 (2008).
24. J. Castilla et al., *EMBO J.* **27**, 2557 (2008).
25. A. J. Raeber et al., *Proc. Natl. Acad. Sci. U.S.A.* **96**, 3987 (1999).
26. R. Gabizon, M. P. McKinley, S. B. Prusiner, *Proc. Natl. Acad. Sci. U.S.A.* **84**, 4017 (1987).
27. We thank A. Aguzzi, M.-S. Sy, and B. Wainer for reagents and A. Steele for comments on the manuscript. Supported by the Ellison Medical Foundation, NIH grant R01NS060729, and Ministry of Education of China project 985.

#### Supporting Online Material

www.sciencemag.org/cgi/content/full/science.1183748/DC1  
Materials and Methods  
Figs. S1 to S14  
Movies S1 to S3  
References

23 October 2009; accepted 18 January 2009  
Published online 28 January 2009;  
10.1126/science.1183748  
Include this information when citing this paper.

## Inhibition of NF- $\kappa$ B Signaling by A20 Through Disruption of Ubiquitin Enzyme Complexes

Noula Shembade,<sup>1\*</sup> Averil Ma,<sup>2</sup> Edward W. Harhaj<sup>1\*</sup>

A20 negatively regulates inflammation by inhibiting the nuclear factor  $\kappa$ B (NF- $\kappa$ B) transcription factor in the tumor necrosis factor receptor (TNFR) and Toll-like receptor (TLR) pathways. A20 contains deubiquitinase and E3 ligase domains and thus has been proposed to function as a ubiquitin-editing enzyme downstream of TNFR1 by inactivating ubiquitinated RIP1. However, it remains unclear how A20 terminates NF- $\kappa$ B signaling downstream of TLRs. We have shown that A20 inhibited the E3 ligase activities of TRAF6, TRAF2, and  $\kappa$ AP1 by antagonizing interactions with the E2 ubiquitin conjugating enzymes Ubc13 and UbcH5c. A20, together with the regulatory molecule TAX1BP1, interacted with Ubc13 and UbcH5c and triggered their ubiquitination and proteasome-dependent degradation. These findings suggest a mechanism of A20 action in the inhibition of inflammatory signaling pathways.

The zinc finger protein A20 (also known as TNFAIP3) has an essential role in limiting the strength and duration of NF- $\kappa$ B signaling (1). A20-deficient mice die prematurely from multiorgan inflammation and cachexia, and

A20-deficient cells exhibit a defect in the termination of tumor necrosis factor- $\alpha$  (TNF- $\alpha$ ) and lipopolysaccharide (LPS)-induced NF- $\kappa$ B signaling (2, 3). A20 requires several regulatory proteins, including Tax1 binding protein

1 (TAX1BP1), and the E3 ubiquitin ligases Itch and ring finger protein 11 (RNF11), to restrict NF- $\kappa$ B activation (4–6). A20 functions as a ubiquitin-editing enzyme with both deubiquitinating (DUB) and ubiquitin E3 ligase activity toward the adaptor protein and death-domain containing protein kinase, receptor-interacting protein 1 (RIP1) in the TNFR pathway (7). A20 first cleaves lysine 63 (K63)-linked polyubiquitin chains on RIP1 and then conjugates lysine 48 (K48)-linked polyubiquitin chains that target RIP1 for degradation by the proteasome (7). A20 also inhibits the polyubiquitination and activation of the E3 ubiquitin ligase TNF receptor-associated factor 6 (TRAF6) in the Toll-like receptor 4 and interleukin-1 receptor (TLR4/IL-1R) pathways

<sup>1</sup>Department of Microbiology and Immunology, Sylvester Comprehensive Cancer Center, The University of Miami, Miller School of Medicine, Miami, FL 33136, USA. <sup>2</sup>Department of Medicine, University of California at San Francisco, San Francisco, CA 94143, USA.

\*To whom correspondence should be addressed. E-mail: nshembade@med.miami.edu (N.S.); eharhaj@med.miami.edu (E.W.H.)